Dilute-defect magnetism: Origin of magnetism in nanocrystalline CeO_2

V. Fernandes,[1] R. J. O. Mossanek,[2] P. Schio,[3] J. J. Klein,[1] A. J. A. de Oliveira,[3] W. A. Ortiz,[3] N. Mattoso,[2] J. Varalda,[2] W. H. Schreiner,[2] M. Abbate,[2] and D. H. Mosca[2]

[1]*PIPE, Universidade Federal do Paraná, 81531-990 Curitiba, PR, Brazil*

[2]*Departamento de Física, Universidade Federal do Paraná, 81531-990 Curitiba, PR, Brazil*

[3]*Departamento de Física, Universidade Federal de São Carlos, 13565-905 São Carlos, SP, Brazil*

(Received 7 October 2008; revised manuscript received 20 March 2009; published 13 July 2009)

We investigate experimentally and theoretically the origin of magnetism in nanocrystalline-undoped ceria films. Our results are consistent with density-functional calculations showing that both oxygen and cerium vacancies lead to ferromagnetism. Although the number of cerium vacancies is smaller than that of oxygen vacancies, the relatively high magnetic moment of the former might result in a substantial contribution to the magnetic properties. Diluted defect magnetism is suggested as a universal feature of ferromagnetism in nonmagnetic oxides without magnetic impurities.

DOI: 10.1103/PhysRevB.80.035202 PACS number(s): 75.10.−b, 71.15.Mb, 71.23.−k, 75.70.−i

I. INTRODUCTION

The search for novel ferromagnetic materials with high Curie temperature for multifunctional spintronics applications has triggered an intense activity on doping of transparent wide-bandgap nonmagnetic oxides with magnetic ions.[1,2] In spite of all the efforts, room-temperature ferromagnetism (RT-FM) observed in some diluted magnetic oxides (DMO) doped with a few percent of a 3*d* cation is not completely understood and remains controversial. Experimental artifacts, segregation of secondary ferromagnetic phases, magnetic clusters, and indirect exchange mediated by carriers[3,4] (electrons and holes associated with impurities) have been invoked to explain the RT-FM in some DMOs, since no long-range order is anticipated below the cation percolation threshold (normally greater than 10%).[2,5] It is strongly believed that the defects in DMOs play a crucial role in inducing ferromagnetism since conventional ideas of magnetism are unable to account for the RT-FM. Due to anisotropic magnetization effects,[6,7] it is quite possible that not only point defects are intervening, but also extended planar defects associated with film surfaces, grain boundaries, and nanocrystalline surfaces. In fact, experimental evidence of ferromagnetism has been reported as an intrinsic property in a number of undoped and nonmagnetic insulating oxides.[8–12] The term d^0 ferromagnetism was suggested to cover these cases.[13] At present, possible mechanisms proposed to explain the unexpected magnetism in this novel class of ferromagnetic materials, where nominal magnetic ions are not present or are not agents, involve point structural defects in crystals such as cation vacancies.[14–16] These point defects have an open-shell electronic configuration, which can indeed confine the compensating charges in molecular orbitals and, under certain conditions, a local magnetic moment will be formed. Nonequilibrium growth conditions and/or the existence of nanocrystalline surfaces are envisaged practical conditions to facilitate magnetic percolation, which requires a minimum of 4.9% vacancies in the case of a face-centered cubic lattice. Electrons trapped in oxygen vacancy (V_O) sites (so-called *F* centers), as in DMOs with oxygen deficiencies,[6,17] have also been suggested as most likely essential to mediate the magnetic coupling.[1,18] In essence, a deeper insight into complex defect physics is necessary to understand the ferromagnetic behavior in these systems.

This work presents electronic and magnetic properties of nanocrystalline undoped CeO_2 (ceria) films electrochemically deposited on silicon. We propose the possibility of intrinsic point defects as the effective source of RT-FM in CeO_2. In contrast to previous reports, we found that not only oxygen vacancies (V_O) are responsible for RT-FM, but also that cerium vacancies (V_{Ce}) contribute to the observed ferromagnetic character. This conclusion is based mostly on experimental results but is also consistent with our density-functional calculations. These calculations show that both V_O and V_{Ce} lead to a ferromagnetic state. Nonequilibrium growth conditions and sample aging suggest that independently on the V_O concentration, RT-FM is strongly affected by the presence of small amounts of V_{Ce} which possess a quite large magnetic moment. This *diluted defect magnetism* (DDM) is preponderant on the stability of the FM ground state, elucidating most of the controversial results observed among nanocrystalline systems and between crystalline and nanocrystalline samples.

II. EXPERIMENTAL

Electrodeposition of ceria films was carried out with a simple stationary three-electrode cell. A saturated Ag/AgCl electrode was used as the reference, whereas the counter electrode was a Pt disk. As already described,[19] ceria films were electrochemically deposited at cathodic potentials of −1.0 and −1.2 V from bidistilled aqueous solutions, containing 800 μmol/L of $CeCl_3.7H_2O$ with and without appropriate amounts of hydrogen peroxide, respectively. The substrates were commercial single-side polished *p*-type Si(001) with electrical resistivity of 10 Ω-cm at RT, which have been hydrogen terminated by removal of the native oxide via chemical HF etching. The samples which were adherent, uniform, and transparent were prepared with thickness ranging from 30 to 250 nm. Here, we denote by sample A deposit with thickness of 30 nm made in pH=5.5–4.5 and samples B and C deposits with thicknesses of 30 and 250 nm, respec-

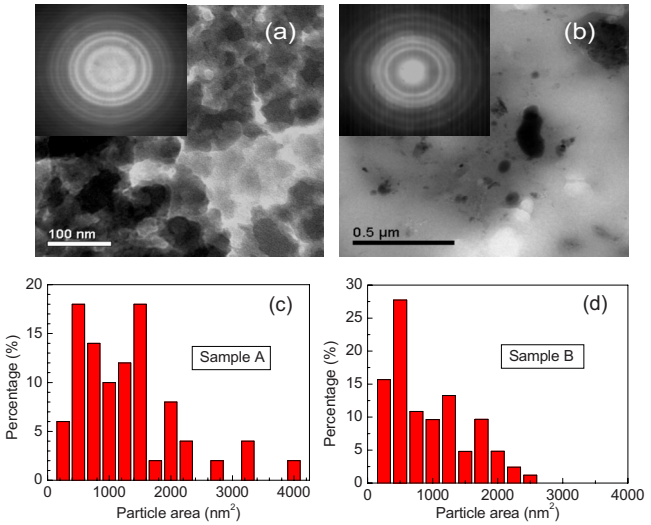

FIG. 1. (Color online) Plain-view TEM images exhibiting the nanocrystalline structure of (a) sample A and (b) sample B. Insets show the corresponding SAED patterns with diffraction rings. The sequence from inner to outer is indexed as (111), (200), (220), (311), (331), (422), and (511) planes for CeO_2 with cubic fluorite-type structure. Histograms of nanocrystallite areas are given to the (c) sample A and (d) sample B.

tively, made in pH=3.5–4.0 by addition of an appropriate amount of hydrogen peroxide to promote an extra oxidized environment. The chemical composition of the deposits was analyzed by x-ray photoelectron spectroscopy (XPS), using a VG ESCA3000 spectrometer, equipped with conventional Mg and Al x-ray sources and a semihemispherical energy analyzer with overall resolution of 0.8 eV, and an energy-dispersive x-ray spectroscopy (EDS) system, using a JEOL JSM 6360-LV electron microscope. Transmission electron microscopy (TEM) images in plain view and corresponding selected-area electron diffraction (SAED) of the deposits were performed using a JEOL JEM 1200EX-II system operating at 120 kV. All magnetic measurements were performed using a Quantum Design MPMS-5S SQUID magnetometer with the magnetic field applied parallel to the film plane.

III. RESULTS AND DISCUSSION

A. Structure, stoichiometry, and magnetic properties of CeO_2 films

Structural characterization of samples A and B are shown in Figs. 1(a) and 1(b), whereas histograms with crystallite areas are shown in Figs. 1(c) and 1(d), respectively. Sample A exhibits a nanocrystalline structure with mean sizes of grains of about 30 nm. Corresponding electron-diffraction patterns are shown as an inset in Fig. 1(a). According to Fig. 1(b), more wide and diffuse rings are observed for sample B, indicating that this deposit includes a significant amount of an amorphous phase with embedded nanocrystals with mean sizes ~25 nm. The interplanar spacings determined from the diffraction-ring diameters for both samples are clearly associated with the Bragg-reflections peaks of CeO_2 having cubic fluorite-type structure with space group of *Fm*-3*m* with a lattice-parameter $a=0.541$ nm. Neither contamination nor intermediate compounds have been detected.

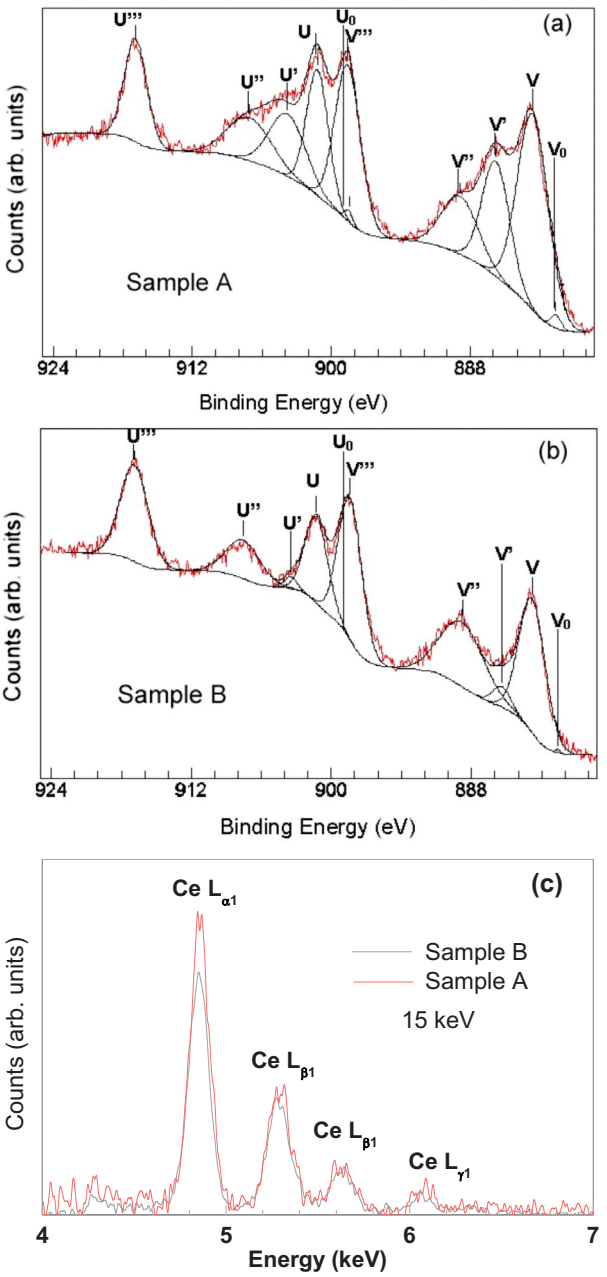

FIG. 2. (Color online) XPS spectra of Ce 3*d* core level for (a) sample A and (b) sample B with spectral contributions used to estimate the amount of O vacancies. (c) Normalized EDS patterns showing *L*-emission line regions for samples A and B indicate different amounts of Ce vacancies in both samples.

XPS Ce 3*d* spectra are illustrated in Figs. 2(a) and 2(b) for both nanocrystalline CeO_2 films. The binding-energy scale was calibrated to that of the Si $2p_{3/2}$ photopeak of bulk Si to correct energy shifts due to charging effects. There are 10 deconvoluted Gaussian-peak assignments in the spectra, where peaks labeled as U, U″, U‴, V, V″, and V‴ refer to $3d_{3/2}$ and $3d_{5/2}$, respectively, and are characteristic of Ce^{4+} 3*d* final states; while U_0, U′ and V_0, V′ refer to $3d_{3/2}$ and

$3d_{5/2}$, respectively, and are present for Ce^{3+} $3d$ final states.[20] The ratio between fitted peak areas of Ce^{4+} and Ce^{3+} for ceria can be used to estimate the contributions of Ce^{4+} and Ce^{3+} valence states and the presence of Ce^{3+} implies the defect structure $CeO_{2-\delta}$ of the film; i.e., reflects the V_O concentration.[19] Our estimate of Ce^{3+}/Ce^{4+} ratio indicates an increase of 3.3% to 22.7% for Sample B prepared in extra oxidizing environment [Fig. 1(b)] compared to Sample A [Fig. 1(a)]. This matches well with the trend expected from the electrochemical experiments, i.e., V_O concentration is higher for sample A than for samples B and C. Our results confirm also that even in the presence of strong deviations from stoichiometry (nominally, $CeO_{1.97}$ for sample B and $CeO_{1.81}$ for sample A) the deposits preserve their fluoride-type structure,[21] as shown by Figs. 1(a) and 1(b). The elemental quantification was also performed using EDS coupled with scanning electron microscopy (SEM). A selected region of the L emission lines for Ce of samples A and B is shown in Fig. 2(c). The EDS spectra were normalized accounting for similar analyzed interacting volumes of the films. From these measurements, we may estimate, by assuming the CeO_2 bulk density, that the V_{Ce} concentration is about 8% higher in sample B than in sample A. For convenience we also assume that V_{Ce} is low to affect the determination of V_O by XPS, although some V_{Ce} is plausible in both samples. In fact, even if oxygen vacancies are indeed the most important native charge-compensating defects over a wide range of conditions, cerium vacancies, oxygen interstitials, and cerium antisites are also important and their roles have largely been neglected in nonstoichiometric nanoceria.[22,23]

Magnetization curves as a function of applied magnetic field (M-H) at 300 K for samples A and B are shown in Fig. 3(a). Both samples are ferromagnetic at 300 K with saturation magnetization (M_S) of 92.6 and 118.4 G for samples A and B, respectively. These values correspond to 1.58 and 1.62 Bohr magnetons per CeO_2 molecule for samples A and B, respectively. The remanences are, respectively, 0.13 M_S and 0.10 M_S for samples A and B, whereas coercive fields have approximately the same value of 110 Oe for both samples. Temperature dependence of the field-cooling magnetization curves for samples A and B with magnetic fields of 1 and 5 kOe are shown in Fig. 3(b). Magnetization slightly diminishes with increase in the temperature, indicating a critical temperature higher than the room temperature. At temperatures below 50 K, the rise of the magnetization suggests the alignment of isolated magnetic moments along with the magnetic field applied. Comparatively to sample A, sample B has a smaller V_O and a somewhat higher V_{Ce} presenting a magnetic moment per CeO_2 higher than that for sample A. In order to get a deeper insight into the V_O influence, we investigated the saturation magnetization values of sample C, which is similar to sample B, although much thicker. The saturation magnetization evolution as a function of storage time under dry atmospheric conditions for sample C is shown in Fig. 3(c). Despite an exponential-like reduction in the saturation magnetization from about 100.0 to 7.0 G along almost two years, this sample stabilizes in a ferromagnetic state at room temperature. XPS analyses clearly reveal a progressive reduction in the oxygen deficiency in the

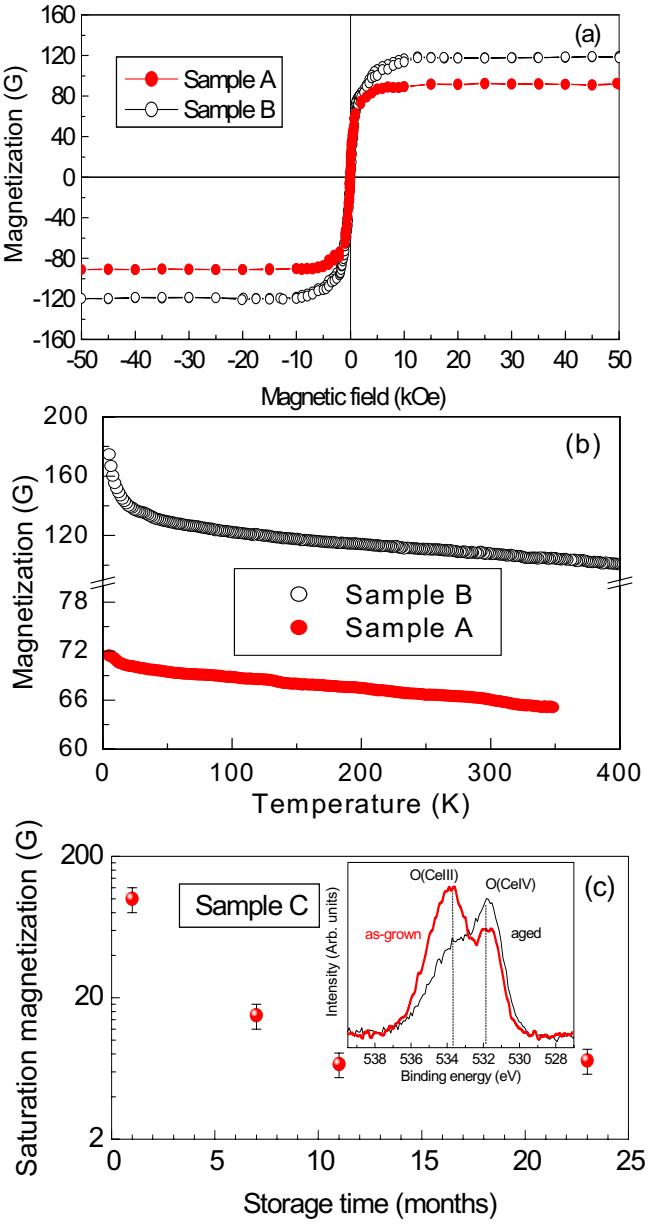

FIG. 3. (Color online) (a) M-H curves at 300 K are shown for samples A and B. (b) Field-cooling magnetization curves for samples A and B taken under magnetic fields of 1 and 5 kOe. (c) Evolution of the saturation magnetization as a function of storage time under ambient conditions for sample C reveals a progressive loss of magnetization. Inset shows XPS O 1s core-level spectra for sample C as-grown and after 24 months storage in air. High- and low-binding-energy components denoted as O(CeIII) and O(CeIV) correspond to oxygen bounded with Ce^{3+} and Ce^{4+} ions, respectively. The energy splitting of these components is ~1.7 eV, as indicated by vertical dashed lines.

sample. The inset in Fig. 3(c) shows the XPS O 1s core-level spectra for sample C as-grown and after 24 months storage at dry atmospheric condition. This result corroborates previous work, reporting that oxygen vacancies in the interior of CeO_2 tend to migrate to the surface,[24] where oxidation can more easily occur. We have observed that annealing effects in O_2 atmosphere (vacuum) can also induce an attenuation (en-

hancement) in the spectral components associated with oxygen bonded with Ce^{3+} ions, denoted by O(CeIII), with respect to oxygen bonded with Ce^{4+} ions, denoted by O(CeIV). This feature is promptly followed by decreasing (increasing) in the saturation magnetization. We take advantage of aging effect which involves low-energy processes comparatively to high-temperature annealing. Aging allows for the mobility of V_O without significant changes on the grain sizes and V_{Ce} positions. Since ferromagnetism in ceria was shown to be connected to grain sizes,[10,18,25] sample aging is more effective than annealing to demonstrate the residual magnetization relationship with V_{Ce}. The observation of residual magnetization is a clear manifestation of DDM, as it strongly indicates the existence of a non-negligible contribution coming from magnetic moments associated with V_{Ce}.

Several works have recently reported RT-FM for single crystalline,[26,27] polycrystalline,[8,28,29] and nanocrystalline.[18] Co-doped CeO_2 thin films, as well as Ni-doped CeO_2 nanoparticles[30,31] and undoped CeO_2 nanoparticles,[10] nanobelts,[25] and nanocubes.[18] For single-crystalline Co-doped CeO_2 thin films, the magnetism depends sensitively on the oxygen pressure during growth and annealing, being the magnetization loss reversible under oxidizing and reducing atmospheres.[27] For CeO_2 nanocubes it was reported that oxygen vacancy-induced moment depends on the location of vacancy.[18] In counterpart, crystalline Ni-doped CeO_2 (Refs. 30 and 31) and undoped CeO_2 (Ref. 10) nanoparticles exhibited magnetism almost independent of V_O. Our experimental findings indicate that both V_{Ce} and V_O amounts are relevant parameters for the ferromagnetic behavior. From this point of view, it is expected that magnetism of crystalline and ordered samples are strongly dependent on V_O since a reduced V_{Ce} amount is determined by the thermodynamics. On the other hand, it is expected that magnetism of nanocrystalline and disordered samples with significant V_O and V_{Ce} amounts could be weakly dependent on V_O due to the contribution of intrinsic ferromagnetism associated with V_{Ce}. The observation of paramagnetism in highly crystalline samples prepared by laser ablation and ferromagnetism in highly disordered samples prepared by electrodeposition[32] are in good agreement with our present explanation. Therefore, our present results shine some light on most of the controversial results currently found by different groups.

B. Band-structure calculations

The origin of ferromagnetism in solids can be described using two opposite approaches: (i) the Heisenberg approach, where the ions have a certain localized moment, which interacts with the moment at the neighbors through an exchange-coupling *J*. This method was used, for instance, by Litvinov to study ferromagnetism in doped GaN,[33] and (ii) the band ferromagnetism approach, where the magnetic moment is delocalized through the solid, and the exchange interaction I splits the majority and minority sub-bands. This method was used, for instance, by Ge *et al.*[18] to study ferromagnetism in CeO_2 nanocubes. Using the second approach, we show that not only O but also Ce vacancies could, in principle, produce ferromagnetism in CeO_2 thin films. The magnetic moment in this method is not localized at the vacancy site, but rather it is delocalized through the entire supercell. It is worth noting that the conclusions are derived from the experimental data, our calculations are just to support these conclusions.

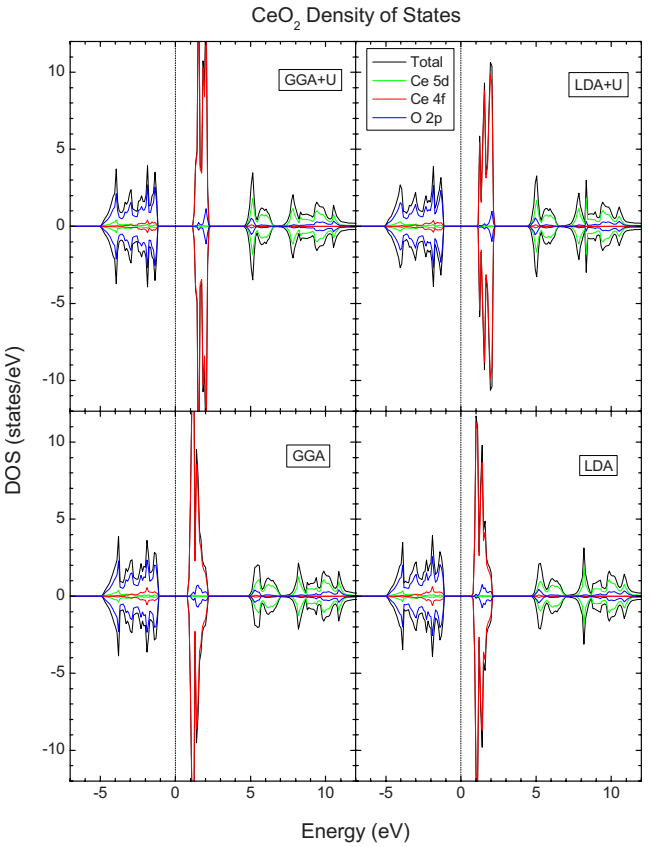

FIG. 4. (Color online) Comparison between the spin-resolved Density of States (DOS) calculated with the LDA, GGA, GGA+U, and LDA+U approaches for stoichiometric CeO_2.

We present here band-structure calculation for stoichiometric CeO_2, as well as for a single Ce or O vacancy in supercells with 4, 8, and 16 CeO_2 units. The resulting Ce and O vacancy concentration was between 3% and 25%, which is in the range of the experimental estimates for our CeO_2 thin films (3.3–27.7 %). Our density-functional theory calculations were performed with the local-density approximation (LDA) and the generalized-gradient approximation (GGA) using the full-potential linear muffin-tin-orbital method (LMTO) code LmtART.[34] The space group of CeO_2 was $Fm\text{-}3m$, the lattice parameter was $a=0.541$ nm, and the atomic positions were Ce ($4a$) (0; 0; 0) and O ($8c$) ($\frac{1}{4};\frac{1}{4};\frac{1}{4}$). The basis set for the (semicore) valence electrons consisted of the ($2s$), $2p$, and $3d$ orbitals for O, and the $6s$, ($5p$), $5d$, and $4f$ orbitals for Ce.

Figure 4 shows the spin-resolved DOS of stoichiometric CeO_2 with the LDA, GGA, LDA+U, and GGA+U approaches, where U=5 eV.[35] We note that the results are similar in all cases, which show that LDA is already a good approximation in this case. The value of the intra-atomic interaction U for Ce $4f$ electrons is relatively large. However, the Coulomb interaction in LDA(GGA)+U is proportional to $\langle n\rangle U$, where $\langle n\rangle$ is the average number of Ce $4f$

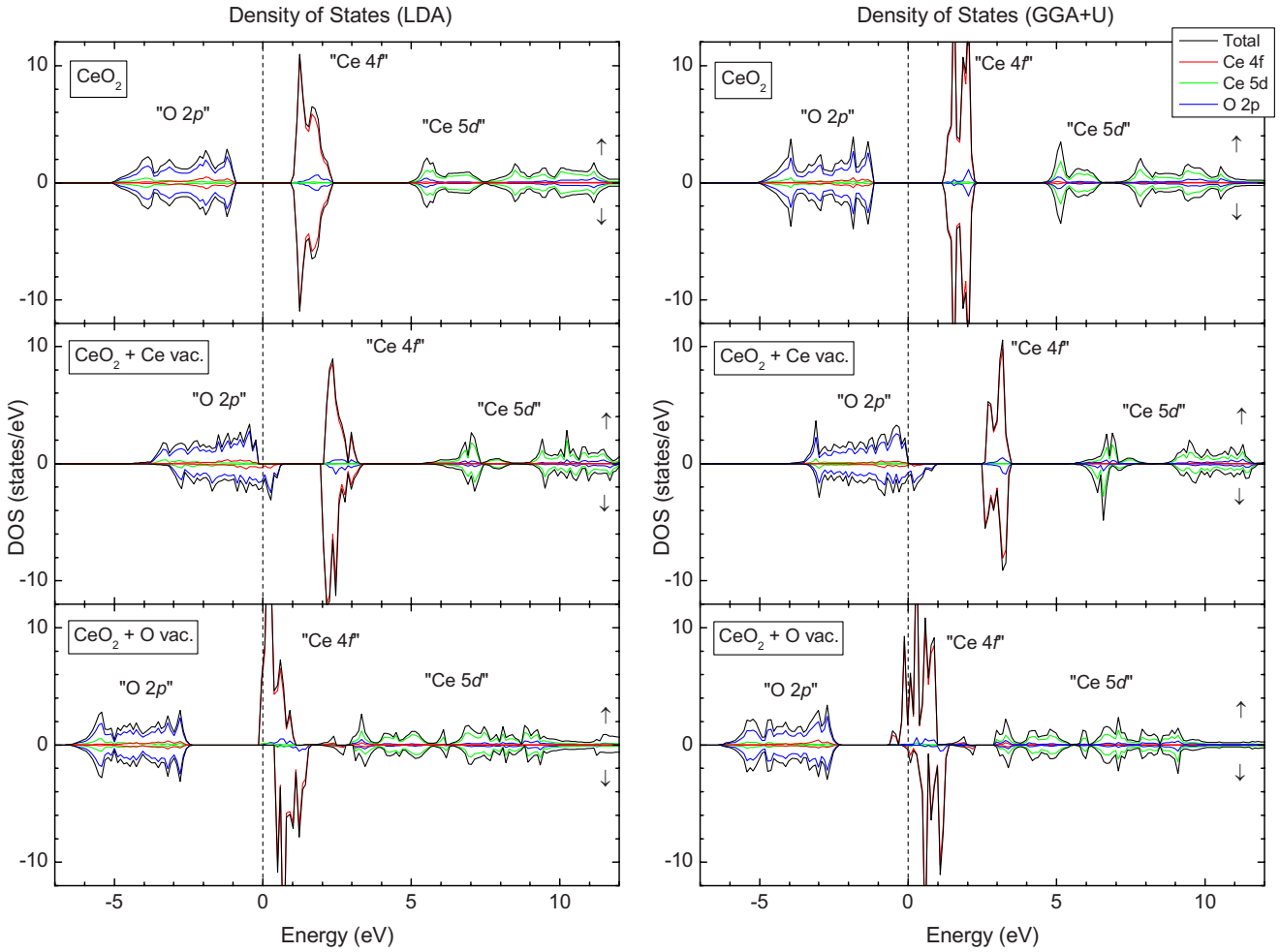

FIG. 5. (Color online) Comparison between the spin-resolved Density of States (DOS) calculated with the LDA and GGA+U approaches for stoichiometric CeO_2, for one Ce vacancy (V_{Ce}) and for one O vacancy (V_O) in a supercell with four CeO_2 units. The total DOS is decomposed into the main (O $2p$, Ce $4f$, and Ce $5d$) partial contributions.

electrons. But the CeO_2 compound is formally a $4f^0$ system and the value of the calculated $\langle n \rangle$ is close to zero.

Figure 5 compares the spin-resolved DOS calculated with the LDA and GGA+U approaches for stoichiometric CeO_2, as well as for one Ce vacancy (V_{Ce}) and for one O vacancy (V_O) in a CeO_2 supercell with 4 formula units. Both calculations show that stoichiometric CeO_2 is a diamagnetic insulator with a bandgap of about 1.8 eV, and is in good agreement with a previous calculation.[36] The results show that the valence band is formed mostly by O $2p$ states, whereas the conduction band is composed mainly by Ce $4f$ and Ce $5d$ states. The presence of a Ce vacancy (V_{Ce}) turns CeO_2 into a ferromagnet with the Fermi level intersecting the minority O $2p$ band. The magnetic moment in this case ($4\mu_B$ per Ce vacancy in both calculations) would be mostly associated with O $2p$ states. On the other hand, the O vacancy (V_O) produces also a ferromagnet with the Fermi level cutting the majority Ce $4f$ band. Now the magnetic moment ($2\mu_B$ per O vacancy in both calculations) would be mainly related to the Ce $4f$ states. The results show again that the LDA calculations already lead to a consistent spin-resolved DOS and magnetic moments even with Ce and O vacancies.

Figure 6 compares the spin-resolved DOS calculated with the LDA approach for one Ce vacancy (V_{Ce}) as well as for one O vacancy (V_O) in different supercells with 4, 8, and 16 CeO_2 units. The band-structure calculations show that the overall density of states does not change much with either the Ce or O vacancy concentration. The results indicate that both the Ce and O vacancies produce a stable ferromagnetic solution for all the calculated vacancy concentrations. The relative energy stabilization of the ferromagnetic phase $\Delta E = E_{para} - E_{ferro}$ for Ce and O vacancies in the different CeO_2 supercells is given in Table I. It is not possible to estimate the value of the critical temperature T_C from a zero-temperature band-structure calculation. However, the calculated energy-stabilizations ΔE for both the Ce and O vacancies are relatively large, and thus compatible with the observed ferromagnetism at room temperature.

Further, the magnetic moment per Ce vacancy ($4\mu_B$) is still associated to O $2p$ states, whereas the magnetic moment per O vacancy ($2\mu_B$) continues to be related to Ce $4f$ states. The sub-band shift I between the majority and minority spins for Ce and O vacancies in the different CeO_2 supercells is listed in Table I. The value of the parameter I is larger for the Ce vacancy and decreases with both the Ce and O vacancy concentrations. If one assumes that the parameter I is related to the effective exchange splitting, then the decrease of I suggests that the magnetic interactions between the vacan-

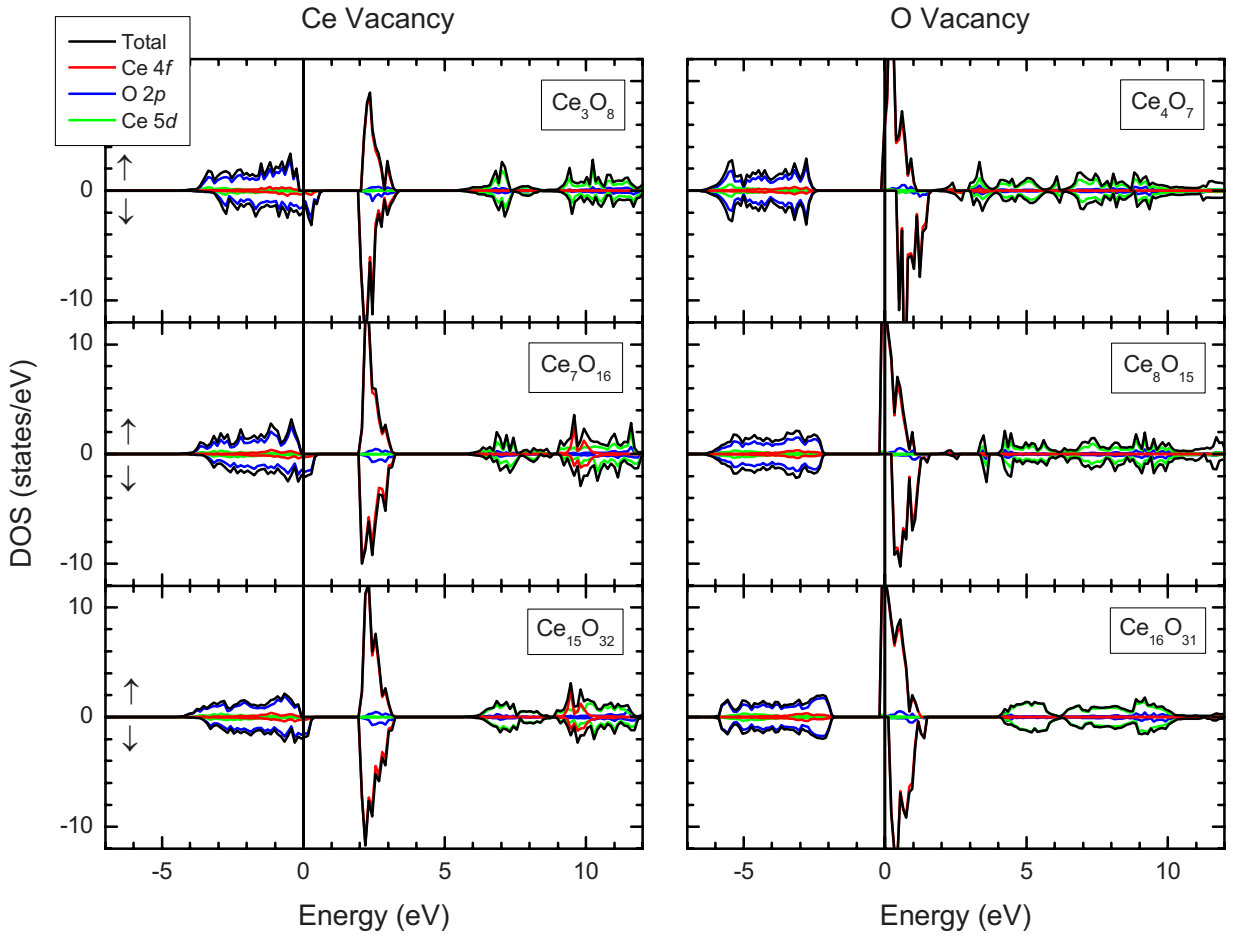

FIG. 6. (Color online) Comparison between the spin-resolved Density of States (DOS) calculated with the LDA for one Ce vacancy (V_{Ce}) and for one O vacancy (V_O) in different supercells with 4, 8, and 16 CeO_2 units. The total DOS is decomposed into the main (O 2*p*, Ce 4*f*, and Ce 5*d*) partial contributions.

cies decreases with the dilution. Interestingly enough, the relative energy stabilization ΔE, the parameter I, and the magnetic moment per vacancy are larger for a Ce than for an O vacancy.

The above band-structure calculations suggest that both Ce and O vacancies could contribute to the observed ferromagnetism in CeO_2. Although thermodynamically the number of Ce vacancies is expected to be smaller than oxygen vacancies, the relatively high magnetic moment of the former would result in a substantial contribution to the magnetic properties. Thus, even a small fraction of Ce vacancies might help to explain the residual magnetization observed for the aged sample, which is not expected to contain a considerable amount of O vacancies, [see Fig. 3(c)]. The interaction between O-O, Ce-Ce, and Ce-O vacancies is a very complex question.[16] Despite the absence of localized paramagnetic centers, our experimental results show ferromagnetism in the diluted limit (~3%). For this reason, we are now mostly interested in the effect of an isolated Ce or O vacancy. As a matter of fact, the magnetic moments associated to the diluted point defects in DDMs would play a similar role to the 3*d* magnetic moments in DMOs.

TABLE I. Relative energy stabilization of the ferromagnetic phase $\Delta E = E_{para} - E_{ferro}$, as well as the sub-band splitting of the DOS I, calculated with the LDA approach for one Ce vacancy (V_{Ce}) and one O vacancy (V_O) in different CeO_2 supercells with 4, 8, and 16 formula units (all values in meV).

	Ce vacancy (V_{Ce})		O vacancy (V_O)	
Formula units	ΔE (meV)	I (meV)	ΔE (meV)	I (meV)
4	−221	726	−159	527
8	−229	595	−148	422
16	−217	476	−138	316

IV. CONCLUSIONS

In summary, our experimental evidences suggest that the observed ferromagnetism in nanostructured CeO_2 is intrinsic, and that magnetic moments are mostly associated with the point defects (Ce and O vacancies) in the structure. Our band-structure calculations indicate that both the Ce and O vacancies are consistent with a ferromagnetic state for all the investigated vacancy concentrations. In conclusion, we show that the presence of diluted defects may be responsible for

the magnetism of nonmagnetic oxides without magnetic impurities, and we think that this effect should be evaluated carefully even for nonmagnetic oxides with magnetic impurities.

Note added. While we were writing the paper, we became also aware of the recent articles of Rahman *et al.*[37] and Soon *et al.*[38] reporting the vacancy-induced room-temperature ferromagnetism in two undoped nonmagnetic oxides (Cu_2O and SnO_2). We agree with the results of these papers based on the same first-principle density-functional calculations used in the present work.

ACKNOWLEDGMENTS

Financial support by the CNPq, CAPES, and FAPESP (Grant No. 2008/10276-5) is acknowledged. The authors thank the technical support of Centro de Microscopia Eletrônica da UFPR.

[1] M. Bibes and A. Barthélémy, IEEE Trans. Electron Devices **54**, 1003 (2007).
[2] J. M. D. Coey, Curr. Opin. Solid State Mater. Sci. **10**, 83 (2006).
[3] J. Philip, A. Punnoose, B. I. Kim, K. M. Reddy, S. Layne, J. O. Holmes, B. Satpati, P. R. Leclair, T. S. Santos, and J. S. Moodera, Nature Mater. **5**, 298 (2006).
[4] A. Kaminski and S. Das Sarma, Phys. Rev. Lett. **88**, 247202 (2002).
[5] S. A. Chambers, Surf. Sci. Rep. **61**, 345 (2006).
[6] M. Venkatesan, C. B. Fitzgerald, and J. M. D. Coey, Nature (London) **430**, 630 (2004).
[7] B. Vodungbo, Y. Zheng, F. Vidal, D. Demaille, D. H. Mosca, and V. H. Etgens, Appl. Phys. Lett. **90**, 062510 (2007).
[8] Y.-Q. Song, H.-W. Zhang, Q.-Y. Wen, L. Peng, and J. Q. Xiao, J. Phys.: Condens. Matter **20**, 255210 (2008).
[9] A. Sundaresan, R. Bhargavi, N. Rangarajan, U. Siddesh, and C. N. R. Rao, Phys. Rev. B **74**, 161306(R) (2006).
[10] Y. Liu, Z. Lockman, A. Aziz, and J. MacManus-Driscoll, J. Phys.: Condens. Matter **20**, 165201 (2008).
[11] N. H. Hong, J. Sakai, N. Poirot, and V. Brizé, Phys. Rev. B **73**, 132404 (2006).
[12] N. H. Hong, J. Sakai, and F. Gervais, J. Magn. Magn. Mater. **316**, 214 (2007).
[13] J. M. D. Coey, Solid State Sci. **7**, 660 (2005).
[14] I. S. Elfimov, S. Yunoki, and G. A. Sawatzky, Phys. Rev. Lett. **89**, 216403 (2002).
[15] C. DasPemmaraju and S. Sanvito, Phys. Rev. Lett. **94**, 217205 (2005).
[16] J. Osório-Guillén, S. Lany, S. V. Barabash, and A. Zunger, Phys. Rev. Lett. **96**, 107203 (2006).
[17] J. M. D. Coey, M. Venkatesan, and C. B. Fitzgerald, Nature Mater. **4**, 173 (2005).
[18] M. Y. Ge, H. Wang, E. Z. Liu, J. Z. Jiang, Y. K. Li, Z. A. Xu, and H. Y. Li, Appl. Phys. Lett. **93**, 062505 (2008).
[19] V. Fernandes, J. J. Klein, N. Mattoso, D. H. Mosca, E. Silveira, E. Ribeiro, W. H. Schreiner, J. Varalda, and A. J. A. de Oliveira, Phys. Rev. B **75**, 121304(R) (2007).
[20] P. Burroughs, A. Hamnett, A. F. Orchard, and G. Thornton, J. Chem. Soc. Dalton Trans. **17**, 1686 (1976).
[21] N. V. Skorodumova, S. I. Simak, B. I. Lundqvist, I. A. Abrikosov, and B. Johansson, Phys. Rev. Lett. **89**, 166601 (2002).
[22] M. Mogensen, N. M. Sammes, and G. A. Tompsett, Solid State Ionics **129**, 63 (2000).
[23] S. Vyas, R. W. Grimes, D. H. Gay, and A. L. Rohl, J. Chem. Soc., Faraday Trans. **94**, 427 (1998).
[24] L. Wu, H. J. Wiesmann, A. R. Moodenbaugh, R. Klie, Y. Zhu, D. O. Welch, and M. Suenaga, Phys. Rev. B **69**, 125415 (2004).
[25] G. R. Li, D. L. Qu, and Y. X. Tong, Electrochem. Commun. **10**, 80 (2008).
[26] A. Tiwari, V. M. Bhosle, S. Ramachandram, N. Sudhakar, J. Narayam, S. Budak, and A. Gupta, Appl. Phys. Lett. **88**, 142511 (2006).
[27] B. Vodungbo, F. Vidal, Y. Zheng, M. Marangolo, D. Demaille, V. H. Etgens, J. Varalda, A. J. A. de Oliviera, F. Maccherozzi, and G. Panaccione, J. Phys.: Condens. Matter **20**, 125222 (2008).
[28] Q.-Y. Wen, H.-W. Zhang, Y.-Q. Song, Q.-H. Yang, H. Zhu, and J. Q. Xiao, J. Phys.: Condens. Matter **19**, 246205 (2007).
[29] L. Bi, H.-S. Kim, G. F. Dionne, S. A. Speakman, D. Bono, and C. A. Ross, J. Appl. Phys. **103**, 07D138 (2008).
[30] A. Thurber, K. M. Reddy, V. Shutthanandan, M. H. Engelhard, C. Wang, J. Hays, and A. Punnoose, Phys. Rev. B **76**, 165206 (2007).
[31] S. K. Misra, S. I. Andronenko, M. H. Engelhard, A. Thurber, K. M. Reddy, and A. Punnoose, J. Appl. Phys. **103**, 07D122 (2008).
[32] Paramagnetic behavior of thinner samples was previously reported in Ref. 19 probably because they were almost fully oxidazed with lower magnetic moment.
[33] V. I. Litvinov, Phys. Rev. B **72**, 195209 (2005).
[34] S. Y. Savrasov, Phys. Rev. B **54**, 16470 (1996).
[35] C. Loschen, J. Carrasco, K. M. Neyman, and F. Illas, Phys. Rev. B **75**, 035115 (2007).
[36] N. V. Skorodumova, R. Ahuja, S. I. Simak, I. A. Abrikosov, B. Johansson, and B. I. Lundqvist, Phys. Rev. B **64**, 115108 (2001).
[37] A. Soon, X.-Y. Cui, B. Delley, S.-H. Wei, and C. Stampfl, Phys. Rev. B **79**, 035205 (2009).
[38] G. Rahman, V. M. García-Suárez, and S. C. Hong, Phys. Rev. B **78**, 184404 (2008).